Multi-source Energy Harvesting for IoT nodes

Philip-Dylan Gleonec, Jeremy Ardouin, Matthieu Gautier, Olivier Berder

Multi-source Energy Harvesting for IoT nodes

Philip-Dylan Gleonec
Wi6labs / University de Rennes 1, IRISA
10 Rue de Jouanet, ePark
35700 Rennes
philip-dylan.gleonec@wi6labs.com

Jeremy Ardouin
Wi6labs
10 Rue de Jouanet, ePark
35700 Rennes
jeremy.ardouin@wi6labs.com

Matthieu Gautier and Olivier Berder
University de Rennes 1, IRISA
IRISA-ENSSAT, 6 rue Kerampont
F-22305 Lannion Cedex
matthieu.gautier@irisa.fr, olivier.berder@irisa.fr

***Abstract*— Power consumption is a primary concern for wireless sensor networks. In order to reduce the use of batteries in these devices, the use of energy harvesting technologies has been considered. Yet, most of the existing solutions rely on a single energy source, thus potentially reducing the sensor reliability. In this paper, we present a circuit which switches between multiple heterogeneous energy sources, and uses a single power conditioning block. A prototype has been developed and validated with an existing wireless sensor platform. Measurements show that switching between energy sources can efficiently combine two energy sources in order to increase device autonomy and/or quality of service.**

I. Introduction

Driven by the trend of the Internet of Things (IoT) and the uninterrupted demand for Machine-to-Machine (M2M) applications, Wireless Sensor Network (WSN) has become an important research area for both academic and industrial worlds. In particular, sensor power efficiency is a particular concern when deploying WSNs, in order to increase their lifecycle and/or their Quality of Service (QoS).

Most of the current sensor nodes are powered by batteries, which limits their available energy. In order to save power, most nodes use duty cycling technique: the device is kept in a low power mode most of the time, and only wakes up for a short time when required. A trade-off has to be made between autonomy and QoS, to define the optimal time between two consecutive wake-ups [1].

In order to maximize the QoS of energy constrained nodes, three main axes have been explored. The first one is the reduction of the node power consumption, through the conception of more energy efficient components [2], and notably more efficient radio protocols [3]. The second one is the optimization of power usage, through the use of power managers [4] [5], which adapt the node behaviour to its energy constraints. Finally, a third way is to increase the energy of node, by scavenging the environment available energy [6].

A node using energy harvesting classically harvests power from a single energy source, e.g. a solar, wind, vibration... The harvested energy is transformed through a power conditioning block, which converts the harvested power in a voltage suitable to charge a battery and to power the node. This power conditioning block has to be adapted to the energy source nature, and can be either a DC/DC voltage converter for continuous current sources such as solar panels or an AC/DC voltage converter for alternative current sources such as wind turbines. The rechargeable battery can be either a Li-Ion battery or a super-capacitor, depending on the storage requirements.

In order to increase the harvested power, two possibilities exist. One can increase the efficiency of the power conversion. The other way is to increase the harvested power by using multiple concurrent energy harvesting devices. In these multi-sources energy harvesting devices, the node is powered from a battery that is recharged from multiple heterogeneous sources. In this paper, we propose a multi-source energy harvesting architecture, which aims for a low cost and flexible implementation with existing energy harvesting devices.

The harvested energy is first stored in energy buffers, which are connected to a generic power conditioning block through a switch matrix. A controller is used to decide which energy source should be connected to the power block. This architecture focuses on the use of a single generic power conditioning block to reduce the platform cost, and is compatible with multiple energy sources and existing sensor nodes. It also enables implementation of intelligent control algorithms

The rest of the paper is organized as follows. In Section 2, the state of the art of multi-sources energy harvesting systems is reviewed. Section 3 describes the proposed system and gives the design choices for each part of the system. Section 4 presents a prototype implementation of our architecture, gives power consumption measurements, and shows its benefits when powering a LoraWan-based platform. Finally, this paper is concluded in Section 5.

II. State of the art

Multiple solutions have been proposed in order to increase the harvested power available for a node. To this aim, [7] proposed a circuit where different energy harvesting devices are set up in series, using a super-capacitor as energy storage. Each energy harvester uses a dedicated voltage transformation step to charge a capacitor. These capacitors are then stacked in series so that their combined voltage is higher than that of the super-capacitor, in order to charge it. The provided measurements come from simulation, and thus have not been validated in real world conditions. [8] proposes another approach by sharing a common voltage converter between multiple harvesting sources. Switches are used to select each energy harvesting source sequentially during a time slot that depends on the source capabilities. However both, approaches

need custom ASIC design, and thus are not suitable for our requirements.

[9] is one of the reference implementation for multi-source energy harvesting sensors. This platform harvests energy from a solar panel and a wind turbine. Each energy source has its own DC/DC converter and Maximum Power Point Tracking (MPPT) circuit in order to maximize efficiency. Each source stores its energy in a capacitor, and all capacitors are connected with diodes to form a reservoir capacitor array. Likewise, [10] uses multiple energy harvesting system, each including its own power conditioning block, to charge a common battery from a solar panel, a wind turbine and a hydroelectric generator. Each power conditioning block is only activated when enough power is harvested. This information is sent to the node, enabling estimation of the harvested power. In a similar manner, [11] proposes the use of IEEE 1451.4-2004 standard for plug and play detection of energy harvesting and storage modules. This work uses a central multiplexer module to interface a node with multiple harvesting modules, which must all include a power conditioning block to provide an intermediate voltage to a central voltage converter, as well as reverse current protection. All these works share the drawback of requiring a dedicated power conditioning circuit per energy harvesting source, thus multiplying the cost and board space required by the solution.

In the industrial world, [12] uses a patented architecture to switch from a primary energy harvester to a secondary source. This system uses a voltage comparison in order to decide which source can provide the highest voltage source. However, some energy sources can provide power but provide small voltages. Moreover, this system only enables the choice of the best energy source at a given time, and does not use the second source.

III. Multiple source switching system

A. System architecture

Our goal is the design of a modular platform to which multiple energy harvesting devices can be connected. The proposed solution must keep a reasonable cost and must use available Components Off-The-Shelf (COTS) in order to ease industrialization. Fig. 1 shows the block diagram of the proposed multi-source switching system. Each energy harvesting source is connected to a capacitor, which acts as an energy buffer while the source is not in use. Each energy buffer is connected to a central Power Management Integrated Component (PMIC) through an electrically-controlled bidirectional switch. The PMIC energy storage replaces the node battery. When an energy buffer is connected to the PMIC, the latter will draw as much current as it can to charge the energy storage and to power the sensor. The energy buffer is thus emptied and another one can be selected through the switch matrix to power the PMIC. A smart controller is used to decide over which switch should be closed at each moment.

However, practical implementation of the switches can limit the voltage range of the energy harvesting source. Using a flexible controller implementation, it can be easy to add a new energy harvesting device.

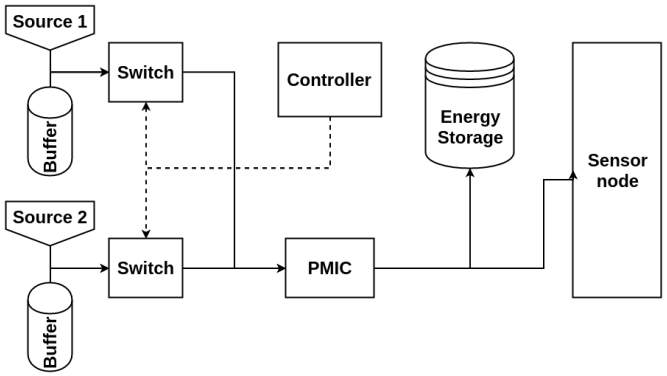

Fig. 1. Multiple source switching system.

One of the main limitations of this architecture is that the power path contains two following DC/DC converters: the first one, embedded in the PMIC, is used to transform the input voltage and to charge the battery, while the second, which is part of the sensor node, takes energy from the battery to power the node components. This approach could be improved as it reduces the overall efficiency of the energy chain from the harvester to the sensor. However, this design choice allows us to easily associate our system to existing sensor nodes, simply by connecting the PMIC battery storage in place of the node one.

Each main function block in the architecture has multiple possible implementations, each one coming with their advantages and limitations. The following subsections detail the role and possible implementations of each main block: energy buffers, controller, PMIC and switches.

B. Power conditioning block

The PMIC is the power manager of the platform. Its main role is to transform the incoming energy in a suitable voltage in order to charge the energy storage (super-capacitor or battery). Implementation can be done with discrete components, using separated circuits for voltage conversion, battery charging and MPPT. Another alternative is to use an Integrated Circuit (IC) which integrates all these functions on the same chip. Both solutions are characterized by low quiescent current and high efficiency at low input power.

Energy harvesting sources present an optimal operating point, called Maximum Power Point (MPP), expressed as the operating voltage V_{MPP} for which the harvested power is maximized. Multiple MPPT techniques have been developed to match the output impedance of the source to the input impedance of the voltage converter, in order to keep the input voltage close to V_{MPP} and thus maximize harvesting efficiency. Without MPPT, the PMIC would pump as much current as it could from the source, making its voltage fall below the minimal input voltage of the PMIC. As V_{MPP} is a constant fraction of the harvester open circuit voltage V_{OC},

a commonly used MPPT technique is to periodically open the circuit to let the harvester reach V_{OC} and to set V_{MPP} according to a measure of V_{OC}.

In the proposed system, this MPPT technique is not applicable, as the energy sources are supposed to store their energy in their buffer, instead of continuously providing power to the PMIC. Thus, when the circuit is opened, the input voltage of the PMIC does not reach V_{OC}, due to the capacitance. Nevertheless, the external voltage V_{MPP} can still be used and set to an arbitrary voltage V_{REF}. The PMIC will then adapt its DCDC switching frequency to keep its input voltage close to V_{REF}. This external control of PIMC can be used by the controller to manage the threshold of the energy buffers.

C. Switch design

Switching between energy sources is a known problem. Power ORing has long been used for applications where power failure is unacceptable, such as datacenters. However, these systems are designed for power consumption of several kW, whereas our application uses only a few mW. Our architecture also requires switches, which can prevent current returns in the harvesters, to avoid damaging them.

Multiple ORing solutions are available. Diodes are the simplest implementation, but their voltage drop and reverse current leakage, coupled with the lack of external control possibility, make them unsuitable for our system. Replacing the diodes with MOSFET transistors avoids the voltage drop, but enables current returns through their reverse diode. Some integrated load switches can prevent reverse current, but their input voltage is often limited.

The switch used in the proposed system in shown in Fig. 2. It is composed of an IC load switch that has no reverse current protection, but both a small size and a low leakage capabilities. A dedicated load switch is selected for each source, depending on its capabilities. Each load switch is coupled with a reverse current protection in the power path. The current protection is implemented by the ideal diode circuit, shown in Fig. 2.

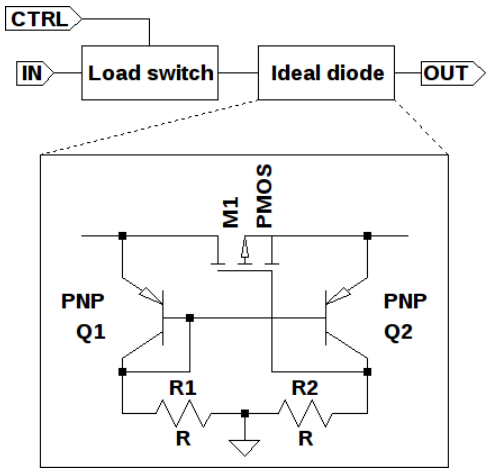

Fig. 2. Load switch block diagram and schematic of the ideal diode circuit.

When the load switch is passing, this circuit has the following behaviour. When the output voltage V_{OUT} is lower than the input voltage V_{IN}, Q2 PNP transistor will be in blocking mode and the FET gate voltage will be 0 V, making it passing. When V_{OUT} is higher than V_{IN}, Q2 is saturated, the gate voltage is close to V_{OUT} and the FET is blocking. The use of two resistors to polarize the PNP transistors creates an additional power consumption. This consumption can be reduced by increasing the resistor values, although the transient response of the circuit is also increased.

D. Controller implementation

In the system, the controller aims at performing the switching process by controlling each switch. Multiple decision algorithms can be implemented depending on the information that the controller could monitor in the system. For example, if the energy levels are known, the controller can allocate a time slot per source that is proportional to its maximum output power. However, as algorithmic considerations are out of the scope of this paper, no information is considered and a passive algorithm is used based on an individual and periodic turn off of each switch. Each buffer is therefore connected to PMIC during a given duration T_{SW}.

The only requirement for the controller is that the control signals must be compatible with the selected switches. The controller is an always-on component, thus its power consumption must be reduced to a bare minimum. Although dedicated analogue or digital circuitry could lower the power consumption of the controller, an ultra low power micro-controller will be used. This allows a good trade-off between power consumption and flexibility.

Indeed, recent micro-controllers usually offer multiple low power modes. By keeping the micro-controller in a low power mode and only waking it up when needed, the average power used by the micro-controller can be kept close to its sleep mode power consumption, *i.e.* few μW. Since the micro-controller functionality is implemented using software, its features can be easily modified, simply by loading a new firmware.

IV. Energy buffer capacitor sizing

A. Analytical model

The input energy buffers are implemented using capacitors. An accurate sizing of theses capacitors is required, as an oversized capacitor would increase its leakage current. On the other hand, an undersized capacitor would be too quickly charged by its energy harvester, leading to energy waste. In the proposed architecture, the size of the input energy buffers depends on both voltage and current provided by the harvesting device, but it depends also on the switching process (*i.e.* number of harvesting devices, period T_{SW} between two decisions, and decision algorithm).

Let C_{BUF} be the buffer capacitance and V_{BUF} its voltage, the current I_{BUF} equation is given by:

$$I_{BUF} = C_{BUF} \frac{d\,V_{BUF}}{dt}. \quad (1)$$

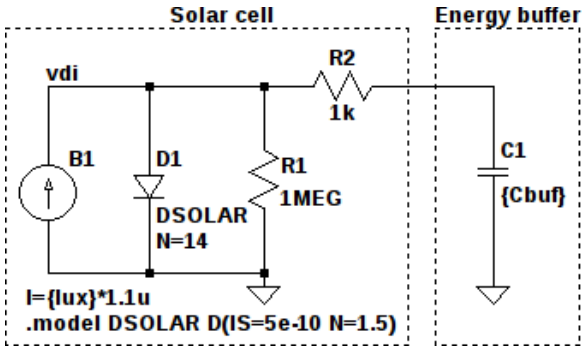

Fig. 3. Simulation circuit for capacitor sizing.

The use of a solar panel is considered, which can provide V_{OC} Volts, I_{MAX} mA and has its MPP at $V_{MPP} = \alpha * V_{MAX}$. At initial conditions, energy buffer is supposed to be empty with a voltage down to V_{REF}. During charging state, once the voltage V_{BUF} reaches V_{MPP}, the power provided by the panel starts to decline. The energy buffer is thus considered to be "charged" when its voltage rises above the V_{MPP} voltage of its harvester. The time t_{CH} required to charge the capacitor up to V_{MPP} is expressed by:

$$t_{CH} = C_{BUF} \frac{\alpha * V_{MAX} - V_{REF}}{I_{BUF}}. \quad (2)$$

As the current I_{BUF} depends on its voltage, the worst case is considered with $I_{BUF} = I_{MAX}$. Over-sizing the current at I_{MAX} leads to the shortest charging time, and thus a biggest capacitance.

The capacitance also depends on the switching process between multiple harvesters. Considering a decision algorithm with a periodic switch between the N sources, one buffer is connected to PIMC during T_{SW}, while being in charging state during $(N-1)T_{SW}$. Therefore, to avoid overcharging the energy buffers in such a scheme, t_{CH} should be greater or equal to $(N-1)T_{SW}$. With this constraint, the minimal energy buffer capacitance C_{BUF} can be computed by:

$$C_{BUF} \geq \frac{T_{SW} * (N-1) * I_{MAX}}{\alpha * V_{MAX} - V_{REF}}. \quad (3)$$

Finally, a safety margin is used to prevent capacitance variations, which can occur according to ambient temperature, input voltage or chosen technology, and which can change over time. This margin can be analytically derived from the capacitor specifications.

B. Model validation

The model for capacitor size calculation has been validated using simulation. This validation step is required by the worst-case approximation we made, supposing that the buffer current is equal to the maximum possible value. Fig. 3 shows the simulation circuit. A buffer capacitor is charged by a simulation model of a solar panel. The light intensity is characterized by its illuminance denoted Ill (in lux). For different capacitances and various illumination conditions, the charge time $t_{CH\ Meas}$ from $V_{REF} = 1.8\ V$ to V_{MPP} is measured, for which the transmitted power is maximal. These results are compared with the theoretical time $t_{CH\ Calc}$ calculated using (2). The comparison of the results is displayed in Table I.

Simulation results show that our model is relatively close to theoretical charge time, especially when the input power increases due to high illuminance. This difference leads to oversize the energy buffers when using the model. This may slightly increase both circuit cost and power losses (due to high leakage currents). However, using a model will speed up the conception time for each configuration of the system.

V. Prototyping and Measurements

A. Implementation

A prototype of the system detailed in the previous section was developed. This implementation aims for functional validation of the platform. The chosen PMIC is a SPV1050 from ST microelectronics, due to its wide input voltage range. This IC integrates a tunable battery charger, and a resistor divider based MPPT circuit. Thus, an external voltage can be applied to manually set the target operating point. If this voltage is not set, the PMIC uses MPPT circuitry, as described earlier.

The implemented load switch is a SiP32431 from Vishay, coupled with the ideal diode circuit described in the previous section. Due to its input voltage limitations, this circuit can only be used for energy harvesting sources providing voltage between 1.1 V and 5.5 V. For different voltages, another load switch would have to be used.

The controller is implemented using an MSP430FR5969 micro-controller from Texas Instruments. Its extensive power modes enable to lower the power consumption of the controller to a few μW. Its flexible clocking trees enable the use of many peripherals while being in low power mode. In our implementation, to avoid adding an external Digital-to-Analogue Converter (DAC), an internal timer is used as a Pulse Width Modulation signal, averaged through an RC filter to provide the PMIC its V_{REF} voltage. V_{REF} is set to 1.1 V, to keep the energy sources voltages in the SiP32421 voltage range. A TPS60210 charge pump with ultra-low quiescent current is used to power the MSP430 with a constant 3.3 V voltage, attenuating the battery voltage variations.

Ill [lux]	C_{BUF} [μF]	$t_{CH\ Meas}$ [s]	$t_{CH\ Calc}$ [s]	Δt_{CH} [%]
100	10	0.262	0.331	26.3
100	100	2.261	3.304	26.0
100	1000	26.214	32.996	25.9
200	10	0.143	0.174	21.6
200	100	1.431	1.755	22.7
200	1000	14.306	17.529	22.5
500	10	0.064	0.074	16.4
500	100	0.636	0.739	16.3
500	1000	6.357	7.374	16.0
1000	10	0.034	0.036	5.3
1000	100	0.342	0.361	5.6
1000	1000	3.418	3.641	6.5

TABLE I

Comparison between measure t_{CHCalc} and model t_{CH} of the charge time.

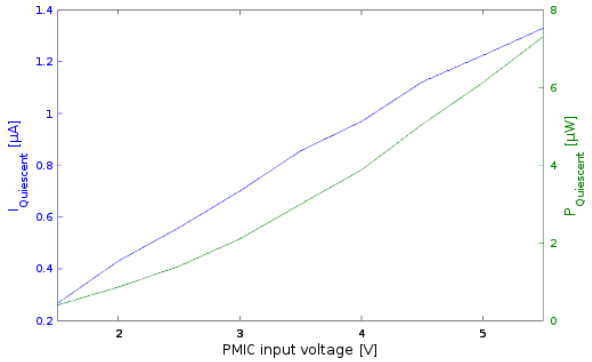

Fig. 4. Quiescent consumption of the PMIC.

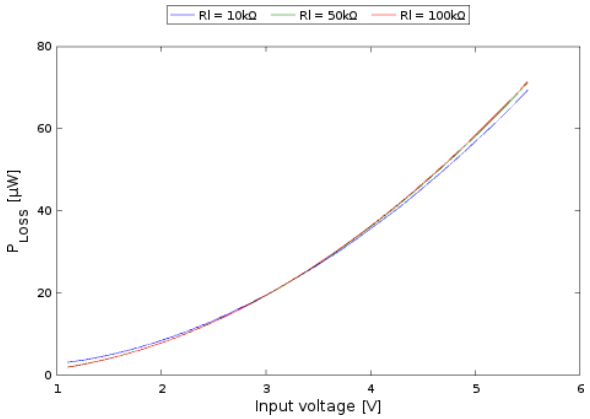

Fig. 5. P_{LOSS} in a passing switch over V_{IN}

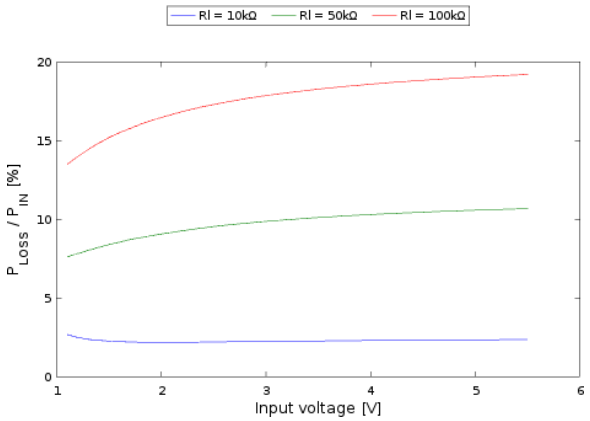

Fig. 6. P_{LOSS} / P_{IN} over V_{IN}

B. Energy consumption overhead

One of the main design goals for the harvester control system is to have a low power consumption in order to not disturb the node energy harvesting capabilities. Thus, power measurements are introduced in this section to ensure that the power consumption overhead of the proposed system is kept low. Since the voltages provided by the different energy harvesters are variable, it is not relevant to measure the current consumption of the system. Instead, power consumption of each block has been separately measured, which can be directly compared with the input power.

1) PMIC power consumption: The PMIC includes some control electronics, and thus has a quiescent current consumption. Since the power consumption overhead of our solution is measured, and not the overall voltage conversion efficiency, the power losses due to the PMIC voltage conversion is not taken in account.

The quiescent current of the SPV1050 is rated at 0.8 μA. Measurements found that this value varied with the input voltage, as shown in Fig. 4. However, the current consumption of the PMIC has little impact compared to the losses in the load switches.

2) Load switch power losses: In order to measure the power losses P_{LOSS} of the load switch, the output power of the switch is subtracted to its input power P_{IN}. Measurements have been made with three different load resistors, for different input voltages V_{IN}. A measurement campaign has also been run while varying the voltage on the switch output, in order to measure its reverse leakage power consumption.

Fig. 5 shows the raw power losses induced by the proposed load switch. In all cases, the power consumption is similar. As most power losses come from the ideal diode circuit resistors, these losses are voltage dependent, and different loads have no impact. However, this also means that the power consumption overhead of the switch is proportionally higher when a lower current is flowing through, as shown in Fig. 6. In our use-case, the current flowing through the switch is reduced when the energy buffer voltage V_{BUF} is close to the reference voltage V_{REF}, *i.e.* when the buffer is nearly depleted.

Moreover, the blocking load switches have a reverse power leakage. Again, these losses are due to the ideal diode resistors, and thus are close to the losses of a passing switch, as shown in Fig. 7 . Adding too many energy harvesting sources has a negative impact on total harvested power, as it increases the total reverse leakage power of the switches. In the case of a system with N energy harvesting devices, the reverse power losses are equal to $(N-1) * P_{LOSS}(V)$.

However, these power losses only affect the currently selected energy harvesting source, which provides current to the PMIC. When the switch is in blocking mode, the other sources are charging their respective energy buffer. Thus, the only power losses that affect them are the leakage current of the energy buffer and the power consumption of the SiP32421 load switch. These power losses are in order of μW, as can be seen in Fig. 8.

3) Controller power consumption: For the controller, MSP430 development platform provides an embedded energy measurement tool. Real-time measurements can be therefore obtained for the power drawn by the controller. In order to take into account the power drawn by the controller charge pump, we powered our development board from the charge pump, and powered this charge pump from the integrated debugger 3.6 V power supply. The charge pump is set in snooze mode through a pull-down resistor, so that its quiescent current consumption is minimized. The State-of-Charge (SoC)

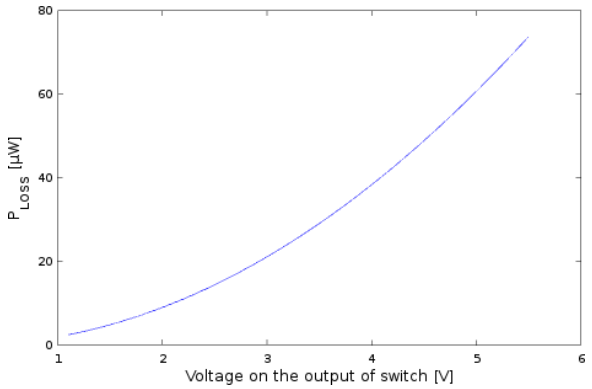

Fig. 7. Reverse P_{LOSS} over V_{OUT}

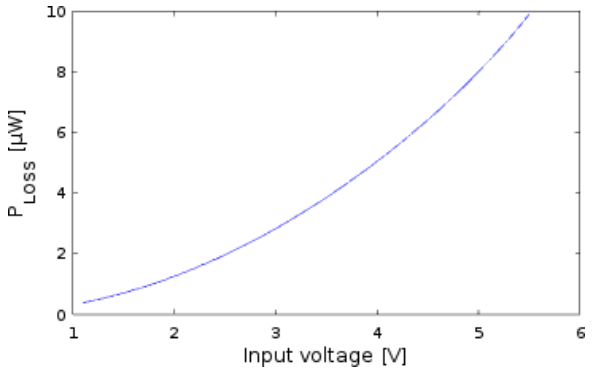

Fig. 8. P_{LOSS} in a blocking switch over V_{IN}

of the main energy storage is measured with an ADC through a resistor divider. An external ADC with high input impedance is used to enhance the measurement precision, and is also powered from the charge pump.

The controller implements a simple decision algorithm, which alternatively closes the switches each $T_{SW} = 1s$. It also implements a simple power manager, which measures the main energy storage SoC and commands the sensor node to transmit a packet. The period between two transmissions T_{PTX} is computed according to the storage charge rate. Therefore, the more energy is harvested, the lower T_{PTX} will be.

Fig. 9 illustrates the power consumption of the controller on a 10 seconds period. To get the average power consumption of the full circuit, we ran a measure for 5 minutes. The mean power consumption was 334 μW for a current of 92 μA. The power losses induced by the controller are relatively high, and mainly come from the ADC measurements required by the power manager. If the switch system is implemented without the power manager, the power consumption of the controller decreases at 185 μW for a current of 51 μA. Although these power losses are low, they could be lowered by integrating the controller functions on the node micro-controller.

C. System validation

1) Test set-up: Our system is used to power a wireless sensor platform developed by Wi6labs company [13]. This platform is built around a STM32 micro-controller from

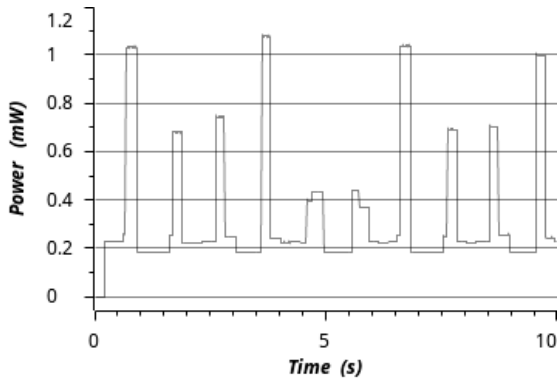

Fig. 9. Power consumption of the controller.

STmicroelectronics, and uses the LoRaWAN protocol for communications. This choice eases the estimation of the power consumption of the node. Indeed, as the LoRaWAN network has a star topology, end device does not have to route any message and its power consumption does not depend on other behaviour of the device.

Voltage generators are used to emulate sources, respectively at 4.2 V and 3.7 V. Both sources are limited to 1 mA in order to simulate low power sources. As the sources are fixed, different measurements can be performed in a consistent set-up, without influence from the environment. However, these sources are oversized compared to real energy sources. As the power provided by real sources would be lower, the power consumption overhead of the circuit would have a higher impact on the harvested energy.

Even if these energy sources are oversized, compared to low power provided by real energy sources, the use of deterministic sources allows an accurate characterization of the proposed system. Different measurements can be performed in a consistent set-up, without being affected by the environment. The input energy buffers used have respectively a 4700 μF and 1000 μF capacitance, while the energy storage is a capacitor array with a 34.7 mF total capacitance.

2) Measurements: The realized prototype shows that the system is able to self-start. Functionality of the controller has also been validated using simple switch algorithms.

In order to compare our proposal against alternatives, several situations are evaluated. S_1 and S_2 correspond to the use of the first and second source alone respectively, connected to the integrated MPPT of the PMIC. D_{MPPT} and D correspond to the two sources both directly connected to the PMIC through the ideal diode circuits, without the switches and energy buffers, respectively with and without the use of the integrated MPPT. In this case, the source with the highest voltage provides current to the PMIC, as only its diode is passing. Due to the current load, the voltage from the source will decrease down to voltage of the second source. At this point, the second diode switches in passing mode, and the second source starts providing current to the PMIC. Both voltages then decrease down to the MPP calculated by the PMIC in situation D_{MPPT}, or V_{REF} in situation D.

Situation	S_1	S_2	D	D_{MPPT}	Reg_{1V1}	Reg_{3V}
$\overline{T_{PTX}}$ [s]	31.3	39.5	67.2	12.3	48.5	21

TABLE II

COMPARISON OF DIFFERENT ENERGY HARVESTING SITUATIONS.

Finally, the switching solution is evaluated as Reg_{1V1}, with the MPPT reference V_{REF} set to 1.1 V. An alternative, Reg_{3V}, uses the same circuit with V_{REF} set to 3.0 V, closer to the source MPP. For all these situations, the period between two transmissions T_{PTX} is measured for ten consecutive packets. The average $\overline{T_{PTX}}$ of these measures are shown in Table II. The higher the power harvested from the sources, the lower $\overline{T_{PTX}}$.

The situation D performs significantly worse than single-source situations, due to the lack of MPPT. This is not the case with D_{MPPT} results. Indeed, because voltages from both sources are close, their V_{MPP} are close too, and the harvested power from both sources is maximized. If the voltages were more different, the total harvested power in D_{MPPT} situation would be lower, and $\overline{T_{PTX}}$ higher. Our proposal, evaluated in situation Reg_{1V1}, performs worse than situation D_{MPPT}, due to the sources operating far from their MPP. However, in situation Reg_{3V}, the PMIC reference voltage V_{REF} was set to operate closer to the MPP, and our solution shows better performance.

As the proposed solution lacks of MPPT, the energy sources operate at a non-optimal operating point, and thus deliver lower power, compared to situation D_{MPPT}. The energy buffer size has also an impact on the system: an oversized buffer takes more time to charge, and the energy source takes a longer time to reach its V_{MPP}. In order to maximize harvesting efficiency, decision algorithms should be designed so that the sources operate near their MPP. An idea would be to set V_{REF} from a DAC and adapt this value in regard of the selected source.

VI. CONCLUSION

This paper describes a multi-source energy harvesting architecture, where multiple energy sources are multiplexed to a single PMIC through a switch matrix. The use of a single voltage converter enables to lower the cost of the solution, while the use of a micro-controller to drive the switches keeps the platform flexible. The system was validated with a real world wireless sensor platform and its power consumption overhead was measured. Measures show our solution can efficiently power a node from multiple energy sources, provided the control algorithm ensure that all sources operate near their MPP. Future work will focus on lowering this power consumption overhead, as well as developing and comparing several algorithms to optimize the switch decision.

REFERENCES

[1] O. Sentieys, O. Berder, P. Quémerais, and M. Cartron, "Wake-Up Interval Optimization for Sensor Networks with Rendez-vous Schemes," in *Workshop on Design and Architectures for Signal and Image Processing (DASIP)*, Nov. 2007.

[2] M. A. Pasha, S. Derrien, and O. Sentieys, "Toward ultra low-power hardware specialization of a Wireless Sensor Network node," in *Proc. 13th IEEE International Multitopic Conference*, pp. 1–6, Dec. 2009.

[3] A. El-Hoiydi and J.-D. Decotignie, "WiseMAC: an ultra low power MAC protocol for the downlink of infrastructure wireless sensor networks," in *Proc. 9th International Symposium on Computers And Communications (ISCC)*, vol. 1, pp. 244–251, IEEE, July 2004.

[4] F. Ait Aoudia, M. Gautier, and O. Berder, "Fuzzy Power Management for Energy Harvesting Wireless Sensor Nodes," in *IEEE International Conference on Communications (ICC)*, May 2016.

[5] T. N. Le, O. Sentieys, O. Berder, A. Pegatoquet, and C. Belleudy, "Power Manager with PID Controller in Energy Harvesting Wireless Sensor Networks," in *IEEE International Conference on Green Computing and Communications*, pp. 668–670, Nov. 2012.

[6] C.-Y. Chen and P. H. Chou, "DuraCap: A supercapacitor-based, power-bootstrapping, maximum power point tracking energy-harvesting system," in *Proc. 16th ACM/IEEE International Symposium on Low Power Electronics and Design (ISLPED)*, pp. 313–318, Aug. 2010.

[7] L. Vijay, K. K. Greeshma, and NS. Murty, "Architecture for ASIC based batteryless multi-source energy harvesting system," in *International Conference on VLSI Systems, Architecture, Technology and Applications (VLSI-SATA)*, pp. 1–6, Jan. 2015.

[8] S. Bandyopadhyay and A. P. Chandrakasan, "Platform Architecture for Solar, Thermal, and Vibration Energy Combining With MPPT and Single Inductor," *IEEE Journal of Solid-State Circuits*, vol. 47, pp. 2199–2215, Sep. 2012.

[9] C. Park and P. Chou, "AmbiMax: Autonomous Energy Harvesting Platform for Multi-Supply Wireless Sensor Nodes," in *Proc. 3rd Annual IEEE Communications Society on Sensor and Ad Hoc Communications and Networks*, vol. 1, pp. 168–177, Sept. 2006.

[10] R. Morais, S. G. Matos, M. A. Fernandes, A. L. Valente, S. F. Soares, P. Ferreira, and M. Reis, "Sun, wind and water flow as energy supply for small stationary data acquisition platforms," *Computers and Electronics in Agriculture*, vol. 64, pp. 120–132, Dec. 2008.

[11] A. S. Weddell, N. J. Grabham, N. R. Harris, and N. M. White, "Modular Plug-and-Play Power Resources for Energy-Aware Wireless Sensor Nodes," in *Proc. 6th Annual IEEE Communications Society Conference on Sensor, Mesh and Ad Hoc Communications and Networks*, pp. 1–9, Jun. 2009.

[12] M. Fall and S. Ajram, "Energy converting apparatus and method," Aug. 1 2012. EP Patent App. EP20,110,290,046.

[13] Wi6labs, "Wi6labs LoRa platform." `http://www.wi6labs.com/lora/`, 2016. [Online; accessed 10-May-2016].